

## Mixing and matching detergents for membrane protein NMR structure determination

Linda Columbus, Jan Lipfert, Kalyani Jambunathan, Daniel A. Fox, Adelene Y. L. Sim, Sebastian Doniach, Scott A. Lesley

### Angaben zur Veröffentlichung / Publication details:

Columbus, Linda, Jan Lipfert, Kalyani Jambunathan, Daniel A. Fox, Adelene Y. L. Sim, Sebastian Doniach, and Scott A. Lesley. 2009. "Mixing and matching detergents for membrane protein NMR structure determination." *Journal of the American Chemical Society* 131 (21): 7320–26. <https://doi.org/10.1021/ja808776j>.



# Mixing and Matching Detergents for Membrane Protein NMR Structure Determination

Linda Columbus,<sup>\*,†,‡</sup> Jan Lipfert,<sup>§</sup> Kalyani Jambunathan,<sup>†</sup> Daniel A. Fox,<sup>†</sup>  
Adelene Y. L. Sim,<sup>||</sup> Sebastian Doniach,<sup>§,||,⊥</sup> and Scott A. Lesley<sup>‡</sup>

Department of Chemistry, University of Virginia, Charlottesville, Virginia 22904, The Joint Center for Structural Genomics and Department of Molecular Biology, The Scripps Research Institute, 10550 North Torrey Pines Road, La Jolla, California 92037, and Departments of Physics and Applied Physics, Biophysics Program, and Stanford Synchrotron Radiation Laboratory, Stanford University, 476 Lomita Mall, Stanford, California 94305

E-mail: Columbus@virginia.edu

## Introduction

Integral membrane proteins comprise  $\approx 25\%$  of most proteomes and facilitate transport and signaling across cell membranes. Despite their importance, less than 1% of known protein structures are of membrane proteins. One major obstacle to membrane protein structure determination is the selection of a detergent that mimics the native lipid bilayer and stabilizes the protein fold.<sup>1–5</sup>

Detergents are small amphipathic molecules that are used to solubilize membrane proteins for structural and functional investigations. However, unlike phospholipid bilayers, detergents form micelles, which are spheroid and have a core composed of the detergent hydrophobic tails. Micelles have different shapes and sizes depending on the detergent chemical structure. For structural investigations, a multitude of detergents is screened until a condition that provides high-quality crystals<sup>3</sup> or NMR

spectra<sup>6</sup> is found. However, a correlation between the physical properties of the detergent micelle and the likelihood of obtaining a membrane protein structure is currently not known.

In this study, we present data on the model polytopic  $\alpha$ -helical membrane protein TM0026. TM0026 is a membrane protein of unknown function from the thermophile *Thermotoga maritima* and was initially characterized as part of the high-throughput structure determination pipeline of the Joint Center for Structural Genomics.<sup>1,7</sup> The data presented demonstrate a correlation between protein conformations, micelle size and thickness, and quality of nuclear magnetic resonance (NMR) spectra. The structure and dynamics of TM0026 in different detergents are investigated by NMR and electron paramagnetic resonance (EPR) spectroscopy and small-angle X-ray scattering (SAXS). The results suggest that matching of the micelle dimensions to the protein's hydrophobic surface avoids exchange processes that reduce the completeness of the NMR observations. Based on these observations, mixed micelles are designed that improve the completeness of NMR observations. These findings provide a basis for the rational design of mixed micelles

<sup>†</sup> University of Virginia.

<sup>‡</sup> The Joint Center for Structural Genomics and Department of Molecular Biology, The Scripps Research Institute.

<sup>§</sup> Department of Physics, Stanford University.

<sup>||</sup> Department of Applied Physics, Stanford University.

<sup>⊥</sup> Biophysics Program and Stanford Synchrotron Radiation Laboratory, Stanford University.

(1) Columbus, L.; Lipfert, J.; Klock, H.; Millett, I.; Doniach, S.; Lesley, S. A. *Protein Sci.* **2006**, *15*, 961–975.

(2) Vinogradova, O.; Sonnichsen, F.; Sanders, C. R. *J. Biomol. NMR* **1998**, *11*, 381–386.

(3) Wiener, M. C. *Methods* **2004**, *34*, 364–372.

(4) Bowie, J. U. *Curr. Opin. Struct. Biol.* **2001**, *11*, 397–402.

(5) Poget, S. F.; Girvin, M. E. *Biochim. Biophys. Acta* **2007**, *1768*, 3098–3106.

(6) Sanders, C. R.; Sonnichsen, F. *Magn. Reson. Chem.* **2006**, *44*, S24–S40.

(7) Lesley, S. A.; Kuhn, P.; Godzik, A.; Deacon, A. M.; Mathews, I.; Kreusch, A.; Spraggon, G.; Klock, H. E.; McMullan, D.; Shin, T.; Vincent, J.; Robb, A.; Brinen, L. S.; Miller, M. D.; McPhillips, T. M.; Miller, M. A.; Scheibe, D.; Canaves, J. M.; Guda, C.; Jaroszewski, L.; Selby, T. L.; Elsliger, M. A.; Wooley, J.; Taylor, S. S.; Hodgson, K. O.; Wilson, I. A.; Schultz, P. G.; Stevens, R. C. *Proc. Natl. Acad. Sci. U.S.A.* **2002**, *99*, 11664–11669.

(8) Hubbell, W. H.; Froncisz, W.; Hyde, J. S. *Rev. Sci. Instrum.* **1987**, *58*, 1879–1886.

that have the potential to advance membrane protein structure determination.

## Experimental Section

**Cloning, Expression, and Purification.** N-terminal His-tagged TM0026 was cloned as previously published.<sup>1</sup> Individual cysteine mutants were produced by standard polymerase chain reaction (PCR) protocols. Protein expression was performed with Luria–Bertani (LB) medium containing 1% glycerol (v/v) and 50 mg/mL ampicillin. Expression was induced by the addition of 0.20% arabinose for 3 h. For deuterated, <sup>15</sup>N-labeled proteins, published protocols using conventional shakers and minimal medium in D<sub>2</sub>O supplemented with <sup>15</sup>NH<sub>4</sub>Cl were used. TM0026 was purified in each detergent (decyl maltoside, DM; dodecyl maltoside, DDM; decylphosphocholine, FC-10; and dodecylphosphocholine, FC-12 from Anatrace, Inc., Maumee, OH; 1-palmitoyl-2-hydroxy-*sn*-glycero-3-[phospho-*rac*-(1-glycerol)], LPPG, and 1,2-dihexanoyl-*sn*-glycerophosphocholine, DHPC, from Avanti Polar Lipids, Inc., Alabaster, AL) as previously described by Co<sup>2+</sup>-affinity chromatography. For cysteine mutants, the lysis and purification buffers contained 0.2 mM tris(2-carboxyethyl)phosphine (TCEP).

TM0026 in the mixed micelles was prepared differently for the two different mixtures investigated. Since TM0026 was soluble in FC-10, TM0026 was purified in FC-10 as above and DDM was titrated into the NMR tube to produce the desired ratio. The feasibility of this strategy indicates that the disruption of the protein structure in FC-10 is reversible and that protein samples may be “rescued” by titrating an appropriate detergent. TM0026 was previously determined to be insoluble in DHPC and yields were low in LPPG;<sup>1</sup> therefore, TM0026 was eluted from the Co<sup>2+</sup>-affinity column with the desired ratio of DHPC/LPPG.

Detergent concentrations were measured by one-dimensional (1D) <sup>1</sup>H NMR by comparison with samples of known detergent concentrations. Protein concentrations were measured by UV absorbance at 280 nm in 6 M guanidine hydrochloride and by bicinchoninic acid (BCA) protein assay (Pierce, Rockford, IL). Detergent solutions for SAXS measurements were prepared in 20 mM phosphate buffer (pH 6.2) and 150 mM NaCl.

**Spin Labeling of TM0026 Cysteine Mutants.** Immediately before spin labeling, TCEP and imidazole were removed by use of a PD-10 desalting column (GE Healthcare Bio-Sciences Corp., Piscataway, NJ) and a 20 mM phosphate buffer (pH 6.2) with 150 mM NaCl and either 5 mM DM, 5 mM DDM, or 15 mM FC-10. Mutant proteins (typically ≈20 μM) were incubated with (1-oxyl-2,2,5,5-tetramethyl-3-pyrroline-3-methyl)-methanethiosulfonate (MTSL; a gift from Wayne Hubbell, UCLA, and Kalman Hideg, University of Pécs) at a 1:5 molar ratio of protein to label. The reaction was allowed to proceed at room temperature overnight. Protein solutions were then concentrated and unreacted spin label was removed by use of a PD-10 desalting column and a 20 mM phosphate buffer (pH 6.2) with 150 mM NaCl and either 5 mM DM, 5 mM DDM, or 15 mM FC-10. The protein eluent was concentrated and spectra were recorded.

**NMR Spectroscopy.** NMR samples were prepared as described previously.<sup>1</sup> The detergent concentrations ranged between 100 and 50 mM, and protein concentrations were ≈0.5 mM. All NMR data were recorded at 313 K on a 600 MHz Bruker Avance spectrometer. Two-dimensional (2D) <sup>15</sup>N,<sup>1</sup>H-TROSY (transverse relaxation-optimized spectroscopy) spectra were recorded with 128 transients per increment,  $t_{1\text{max}}(^{15}\text{N}) = 42$  ms,  $t_{2\text{max}}(^1\text{H}) = 285$  ms, and a time domain data size of 64 ( $t_1$ ) × 2048 ( $t_2$ ) complex points. For the sequence-specific resonance assignments of the polypeptide backbone atoms, the following experiments were recorded: <sup>15</sup>N,<sup>1</sup>H-TROSY, TROSY-HNCA, and <sup>15</sup>N-resolved <sup>1</sup>H,<sup>1</sup>H-NOESY (nuclear Overhauser effect spectroscopy) ( $\tau_m = 200$  ms). By use of the backbone assignment and the <sup>15</sup>N-resolved <sup>1</sup>H,<sup>1</sup>H-NOESY, the protein–detergent complex was modeled based on the observed NOEs between the protein amide protons and the alkyl chains of the detergent.

**Electron Paramagnetic Resonance Spectroscopy.** EPR spectra were recorded on a Varian E-109 spectrometer fitted with a two-loop one-gap resonator.<sup>8</sup> Protein samples of 5 μL (≈100 μM) were loaded in Pyrex capillaries (0.84 mm o.d. × 0.6 mm i.d.) sealed on one end. All spectra were acquired with 2 mW incident microwave power. The modulation amplitude at 100 kHz was optimized for each spectrum to avoid spectral distortion. All spectra were normalized to the same area. All labeled mutants lacked spin–spin interaction, indicating that the protein is monomeric in all detergent conditions, in agreement with previously published results.<sup>1</sup>

**Small-Angle X-ray Scattering.** SAXS data were recorded on beamline BESSERC CAT 12-ID at the Advanced Photon Source, employing a 2 m sample–detector distance and a charge-coupled device (CCD) detector read out. The measurements were performed at a photon energy of 12 keV with a custom-made cell.<sup>9</sup> For each data point, a total of three measurements of 0.5 s integration time were recorded. Data were image-corrected and circularly averaged; the three profiles for each condition were averaged to improve signal quality. Buffer profiles were collected by identical procedures and subtracted for background correction. Radiation damage was tested for by comparing subsequent exposures of the same sample, and no change was detected.

**Modeling of TM0026 in Micelles.** The protein backbone atoms were assigned by use of HNCA and HN(CO)CA 3D spectra.<sup>10</sup> The DDM/FC-10 mixed micelle condition, where 59 out of 68 residues could be assigned (M1–A5, P31, P46, K57, and K58 were not assigned), allowed assignment of 11 additional residues compared to DM. By use of the paramagnetic relaxation enhancement (PRE) measurements from A13R1 (in combination with the backbone assignment), several low-resolution models of the protein structure were calculated.<sup>11–13</sup> A conformation from one of these calculations was used to model the protein–detergent complex. High-resolution structure determination is in progress and will be published elsewhere. The micelles were approximated by use of the headgroup–headgroup spacing and the aggregation number determined by SAXS and the three-dimensional (3D) <sup>15</sup>N-edited NOESY spectrum (Figure S9 in Supporting Information), which provided the amino acids that were within 5 Å of the alkyl chain of the detergent molecules. For the FC-10 micelle, the α-helices were moved as rigid bodies to match the hydrophobic surface area to the micelle dimensions and the termini were exposed to aqueous solvent. Pymol<sup>14</sup> was used to build the protein detergent models and render all protein figures.

## Results and Discussion

TM0026 contains two transmembrane α-helices and was found to be α-helical, monodisperse, and monomeric in four different detergents: DM, DDM, FC-10, and FC-12.<sup>1</sup> Despite these similarities, the NMR signals were drastically different as assessed by the <sup>15</sup>N,<sup>1</sup>H-TROSY spectra (Figure 1).<sup>1</sup> For the detergents DM and FC-12, 51 of 66 expected cross peaks were observed, while for the detergents FC-10 and DDM, only 32 and 36 cross peaks were observed, respectively. When observable, the cross peaks have similar chemical shifts in each detergent micelle, suggesting that the protein structures are similar in the different detergents (Figure 1). The remaining expected cross peaks are not observed in DDM and FC-10

(9) Lipfert, J.; Millett, I. S.; Seifert, S.; Doniach, S. *Rev. Sci. Instrum.* **2006**, *77*, 046108.

(10) Bax, A.; Grzesiek, S. *Acc. Chem. Res.* **1993**, *26*, 131–138.

(11) Battiste, J. L.; Wagner, G. *Biochemistry* **2000**, *39*, 5355–5365.

(12) Schwieters, C. D.; Kuszewski, J. J.; Clore, G. M. *Prog. Nucl. Magn. Reson. Spectrosc.* **2006**, *48*, 47–62.

(13) Schwieters, C. D.; Kuszewski, J. J.; Tjandra, N.; Clore, G. M. *J. Magn. Reson.* **2003**, *160*, 65–73.

(14) DeLano, W. L. Pymol; DeLano Scientific, Palo Alto, CA, 2002; [www.pymol.org](http://www.pymol.org).

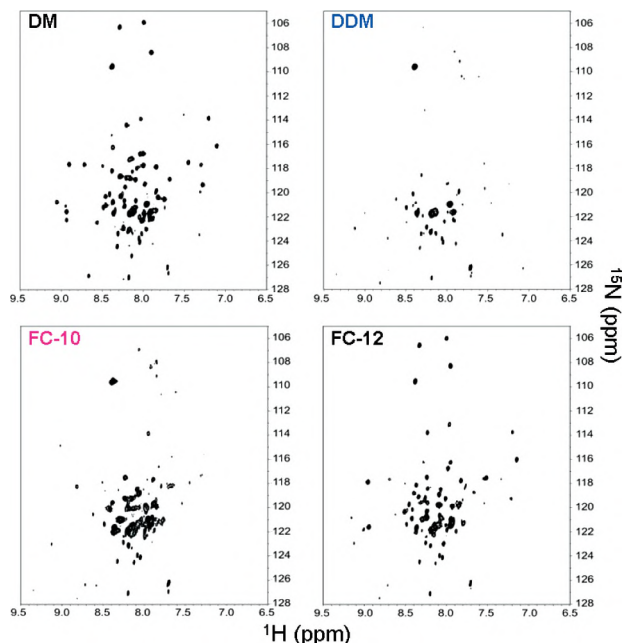


**Figure 1.** Soluble protein–detergent complexes differ in conformational heterogeneity. NMR  $^{15}\text{N}$ , $^1\text{H}$ -TROSY spectra of  $^2\text{H}$ , $^{15}\text{N}$ -labeled TM0026 in DM, DDM, FC-10, and FC-12 are shown.

because of extensive line broadening. The observed line broadening, which impedes NMR structure determination, is attributed to conformational heterogeneity and exchange processes and not to aggregation, unfolding, or overall size of the protein–detergent complex.<sup>1,15</sup>

**Structural Changes of TM0026 in Different Detergents.** To investigate the physical origin of the line broadening, site-directed spin labeling (SDSL) was employed to study the structure and dynamics of TM0026 under different detergent conditions. A nitroxide probe (R1, Figure S1 in Supporting Information) was introduced at four sequential sites (Figure 2). These four residues were chosen because they compose a full  $\alpha$ -helical turn at the center of the first hydrophobic sequence and at least one of the residues is likely to be involved in tertiary interactions with the second  $\alpha$ -helix. The introduction of the nitroxide side chain does not significantly perturb the overall structure of TM0026, as the  $^{15}\text{N}$ , $^1\text{H}$ -TROSY spectrum of the protein labeled with R1' (a diamagnetic analogue) is identical to that of wild type (Figure S2 in Supporting Information). The spectral parameters  $\Delta H_{\text{pp}}$  and  $2A_{\text{zz}}$  (Figure 2) provide an assessment of mobility (the central line width,  $\Delta H_{\text{pp}}$ , is determined by the  $g$ -tensor anisotropy; that is, nitroxide mobility modulates the averaging of the  $g$ -tensor elements and reduction in mobility resolves the anisotropies and the line width is broadened) and can be used to determine the topology<sup>16</sup> and backbone dynamics<sup>17</sup> of the  $\alpha$ -helix.

In DM, the EPR spectra of residues L14–L16 are very similar to those observed for R1 at lipid/detergent-exposed sites.<sup>18,19</sup>

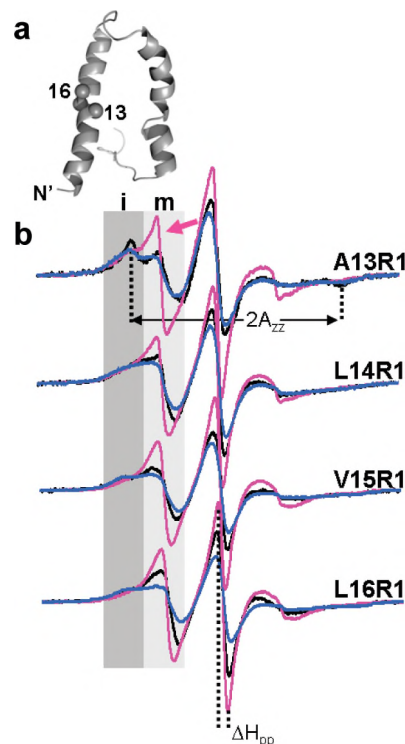


**Figure 2.** Effects of detergent on protein structure and dynamics. (a) Ribbon model of TM0026, with spin-labeled residues A13–L16 represented by spheres (see Experimental Section for modeling). (b) EPR spectra of R1 at residues A13–L16 in DM, DDM, and FC-10, colored according to the labels in Figure 1. Spectral intensities in regions labeled i (dark gray) and m (light gray) identify relatively immobile and mobile components, respectively. The arrow indicates a dynamic population observed in FC-10. The semiquantitative measurements  $\Delta H_{\text{pp}}$  and  $2A_{\text{zz}}$  are indicated.

In contrast, the EPR spectral line shape of A13R1 represents a highly restricted nitroxide side chain, based on the evaluation of  $\Delta H_{\text{pp}}$  and  $2A_{\text{zz}}$  (Figure 2 and Table S1 in Supporting Information), indicating a direct interaction with the second transmembrane  $\alpha$ -helix. In contrast, in FC-10 the EPR spectrum of A13R1 has two components, indicating that R1 samples two conformations. One spectral component is similar to that observed in DM and the other represents a more mobile R1 (Figure 2) and is similar to spectra observed in highly dynamic sequences.<sup>17,20</sup> An increase in mobility for a fraction of the protein population is observed at each labeled position throughout the  $\alpha$ -helical turn. These data suggest that the tertiary interaction between the two  $\alpha$ -helices is lost in a substantial fraction ( $\approx 10$ – $20\%$ ) of the protein population. The structural heterogeneity and potential exchange between the two populations provide a possible explanation for the observed NMR line broadening in FC-10 detergent micelles. In DDM, the tertiary contact at A13R1 is maintained (Figure 2). However, compared to DM, the EPR spectra for the lipid-exposed residues exhibit extensive line broadening as assessed by  $\Delta H_{\text{pp}}$  (the most dramatic difference is observed at L16R1) (Table S1 in Supporting Information). These data demonstrate that the structure of TM0026 is perturbed in FC-10 and DDM; in order to understand how the detergent influences the protein structure, the characteristics of the detergents were investigated.

**Comparison of DM, FC-10, DDM, and FC-12 Micelles.** A comparison of the detergent properties (Table 1, Figure S3 and

(15) Lipfert, J.; Columbus, L.; Chu, V. B.; Doniach, S. *J. Appl. Crystallogr.* **2007**, *40*, S235–S239.

(16) Hubbell, W. L.; Gross, A.; Langen, R.; Lietzow, M. A. *Curr. Opin. Struct. Biol.* **1998**, *8*, 649–656.

(17) Columbus, L.; Hubbell, W. L. *Trends Biochem. Sci.* **2002**, *27*, 288–295.

(18) Altenbach, C.; Marti, T.; Khorana, H. G.; Hubbell, W. L. *Science* **1990**, *248*, 1088–1092.

(19) Gross, A.; Columbus, L.; Hideg, K.; Altenbach, C.; Hubbell, W. L. *Biochemistry* **1999**, *38*, 10324–10335.

(20) Columbus, L.; Hubbell, W. L. *Biochemistry* **2004**, *43*, 7273–7287.



**Table 1.** Properties of Select Detergents

detergent (abbreviation)	cmc (mM)	$N^a$	$L^b$ (Å)	$r_{HC}^c$ (Å)	$V_{HC}^d$ (nm <sup>3</sup> )
<i>n</i> -decyl $\beta$ -D-maltoside (DM)	1.8	80–90	34	12.5, 23	26
<i>n</i> -dodecyl $\beta$ -D-maltoside (DDM)	0.17	135–145	39	14, 29	49
<i>n</i> -decylphosphocholine (FC-10)	11	45–53	28	21, 13	15
<i>n</i> -dodecylphosphocholine (FC-12)	1.5	65–80	34	26, 16	27
1,2-dihexanoyl- <i>sn</i> -glycerophosphocholine (DHPC)	15	30–35	23	21, 10	8.8
1-palmitoyl-2-hydroxy- <i>sn</i> -glycero-3-[phospho- <i>rac</i> -(1-glycerol)] (LPPG)	0.018	160–170	46	19, 30	72
DDM/FC-10	nd <sup>e</sup>	77	34	14, 21	26
(molar ratio 4:7)		(30/47)			
DHPC/LPPG	nd <sup>e</sup>	80	35	17, 20	29
(molar ratio 1:1)		(40/40)			

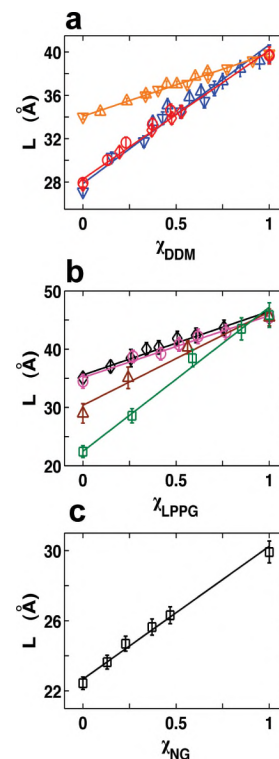
<sup>a</sup> Aggregation number determined by SAXS.<sup>21</sup> <sup>b</sup> Dominant distance from headgroup to headgroup across the short dimension of the micelle core. <sup>c</sup> Radii defining spheroid with one axis *a* and two other axes *b*. <sup>d</sup> Hydrophobic volume calculated from  $r_{HC}$ . <sup>e</sup> Not determined.

Table S2 in Supporting Information) indicates that the detergents that produce resolved NMR spectra (DM and FC-12) do not have similar head groups, ionic properties, or alkyl chain lengths. To characterize the micelles formed by the different detergents, we have determined their shape and size using SAXS. In particular, we obtain the aggregation number (*N*) and hydrophobic core volume ( $V_{HC}$ ) from fits of a two-component spheroid model, and the dominant headgroup separation (*L*, the distance between the head groups centers across the short diameter of the spheroid) from the position of the second maximum in the scattering intensity (see ref 21 and Figure S4 in Supporting Information). We find that DM and FC-12 form micelles of similar size with respect to *N*,  $V_{HC}$ , and *L* (Table 1).<sup>21</sup> In contrast, the detergents for which poor NMR spectra were observed form either smaller and thinner (FC-10) or larger and thicker (DDM) micelles compared to DM and FC-12.

**Dimensions of Mixed Micelles.** In order to further probe the relationship between micelle size and thickness and membrane protein conformational homogeneity, it is desirable to be able to systematically influence micelle geometries. Therefore, we explored whether engineering mixed micelles by mixing detergents at different ratios might be a way to systematically change the size and shape of detergent micelles. To this end, we obtained SAXS data for a comprehensive set of mixed micelles, including detergents with varying hydrophobic tails and head groups, including nonionic, zwitterionic, and ionic species (Figure 3, Figures S4–S6 and Tables S2 and S3 in Supporting Information). The dependence of *L* (determined from the position of the second peak in the scattering intensity) on the mixed micelle composition for two detergents A and B was fit by the relationship

$$L(\chi_A) = L_B + (L_A - L_B)\chi_A \quad (1)$$

with the mixing ratio  $\chi_A = ([A])/([A] + [B])$  (Figure 3, solid lines). [A] and [B] are the detergent concentrations that have been corrected for the monomeric detergent concentration by use of the relationship  $X_{i, \text{monomer}} \approx X_i \text{cmc}_i$ , where  $X_i$  and  $\text{cmc}_i$  are the mole fraction and critical micelle concentration of detergent species *i*.<sup>22</sup> The linear dependence of *L* on the mixing ratio  $\chi$  appears to hold for a wide range of detergent mixtures (Figure 3). The data set includes mixtures of detergents that differ only by their alkyl chain length (DDM/DM mixtures) and that feature different nonionic head groups (DDM/OG mixtures, a mono- and a disaccharide) and combinations of nonionic and



**Figure 3.** Micelle thickness *L* for mixed micelles depends linearly on the mixing ratio. Micelle thickness is plotted as a function of mixing ratio determined from SAXS analysis (symbols) and fits to the linear model (eq 1, solid lines). (a) Mixed micelles of DDM mixed with octyl glucoside (blue triangles), DM (orange triangles), or FC-10 (red circles). (b) Mixed micelles of LPPG mixed with FC-12 (black diamonds), DM (magenta circles), FC-10 (brown triangles), and DHPC (green squares). (c) Mixed micelles of nonyl glucoside and DHPC (black squares).

zwitterionic head groups (DDM/FC-10 and NG/DHPC mixtures), as well as combinations involving an ionic detergent species (LPPG). Furthermore, the relationship of thickness to mixing ratio is largely independent of whether the concentration of detergent A was held fixed and varying concentrations of detergent B were added or whether the reverse strategy was employed. Finally, the relationship seems to be largely independent of the total (absolute) concentration of detergents employed (data not shown), in agreement with the finding that the position of the second peak is independent of detergent concentration for micelles formed by a single detergent species.<sup>21</sup>

**Design of Mixed Micelles for NMR Structure Determination.** The linear dependence of the characteristic micelle thickness on detergent mixing ratios (eq 1) provides a straightforward method to engineer micelles of a particular thickness

- (21) Lipfert, J.; Columbus, L.; Chu, V. B.; Lesley, S. A.; Doniach, S. *J. Phys. Chem. B* **2007**, *111*, 12427–12438.  
 (22) Tanford, C. *The hydrophobic effect: formation of micelles and biological membranes*, 2nd ed.; Wiley: New York, 1980.

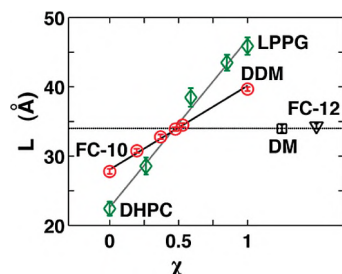


**Figure 4.** Optimization of mixed micelles for TM0026 NMR measurements. Characteristic micelle thickness  $L$  is plotted as a function of the mixing ratio of detergents  $\chi$  for DDM/FC-10 (red circles) and LPPG/DHPC (green squares) mixed micelles. A horizontal line is drawn at the  $L$  value measured for DM and FC-12 (34 Å).

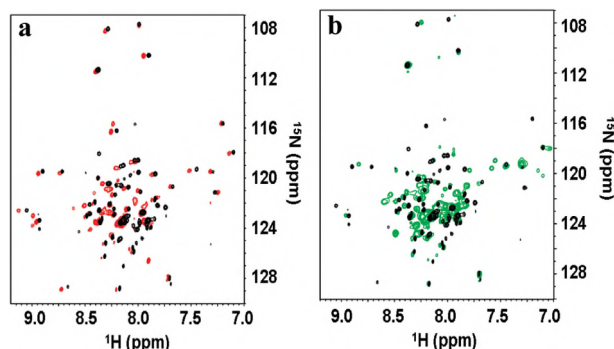


**Figure 5.** NMR  $^{15}\text{N}$ ,  $^1\text{H}$ -TROSY spectra of  $^2\text{H}$ ,  $^{15}\text{N}$ -labeled TM0026 in (a) DDM/FC-10 mixed micelle ( $\chi_{\text{DDM}} \approx 0.4$ , red) and (b) DHPC/LPPG mixed micelle ( $\chi_{\text{LPPG}} \approx 0.5$ , green). In both panels, the spectrum of TM0026 in DM is shown in black.

by mixing detergents. We explored this strategy to test how micelle size and thickness influence protein structure in the context of TM0026. Two mixtures were pursued further for NMR structure determination: DDM/FC-10 and LPPG/DHPC. The DDM/FC-10 pair was chosen as an extension of the four detergents investigated with NMR and SDSL. The LPPG/DHPC mixture was chosen because TM0026 in the individual pure micelles was either insoluble (DHPC) or yielded very poor NMR spectra (LPPG)<sup>1</sup> and, therefore, was a test of the general applicability of the method. Both DDM/FC-10 and LPPG/DHPC micelles have dimensions  $L$ , as well as  $V_{\text{HC}}$  and  $N$ , similar to those of DM and FC-12 at mixing ratios of  $\chi_{\text{DDM}}$  or  $\chi_{\text{LPPG}} \approx 0.4$ – $0.5$  (Figure 4, Table 1, and Table S3 in Supporting Information).

**TM0026 in Mixed Micelles with a Matched  $L$  Parameter.** Figure 5 shows  $^{15}\text{N}$ ,  $^1\text{H}$ -TROSY spectra of TM0026 in DDM/FC-10 and LPPG/DHPC mixed micelles with thicknesses engineered to match the thickness of pure FC-12 or DM micelles, 34 Å. The  $^{15}\text{N}$ ,  $^1\text{H}$ -TROSY spectra of TM0026 in these mixed micelles are similar (with respect to both chemical shift and line broadening) to the spectra in DM and FC-12, indicative of an identical global fold (Figure 5). The EPR spectra of A13R1–L16R1 in the DDM/FC-10 mixed micelle were identical to those observed in DM, suggesting similar tertiary interactions (Figure S7 in Supporting Information). In fact, the quality of the NMR spectra in DDM/FC-10 mixed micelles was such that several additional cross peaks were observed, which facilitated the assignment of 11 additional residues compared to DM, providing a more complete backbone assignment.

**Protein–Detergent Interactions.** NMR NOEs and chemical shift perturbation mapping<sup>23,24</sup> have been widely used to investigate protein–protein and protein–ligand interactions and can provide information about protein–detergent interactions. The backbone assignments of TM0026 in DM and DDM/FC-10 allow a direct comparison of the chemical shifts in each detergent condition. The chemical shift differences  $\{\Delta\delta = [(\Delta\delta_{\text{N}}/5)^2 + (\Delta\delta_{\text{H}})^2]^{1/2}\}$  between the DM and DDM/FC-10 detergent conditions were calculated and, as expected from the overall similarity of the spectra, the majority of the chemical shift differences (Figure S8 in Supporting Information) are small ( $\Delta\delta < 0.4$  ppm, the average chemical shift difference). However, two regions of the protein exhibit greater differences in chemical shifts: L48–R54 and E61–R68 (the protein sequence is shown in Figure S9 in Supporting Information). The variability in the chemical shifts in the C-terminus (E61–R68) might stem from different interactions of the highly charged C-terminus with the zwitterionic FC-10 headgroups compared to the neutral DM head groups. The residues C-terminal of P46 in the second transmembrane helix (L48–R54) exhibit an increased variability in chemical shift. It is plausible that the proline residue results in a kink that uncouples the motion of these residues from the N-terminal region of the helix. The C-terminal region may adopt slightly different conformations in DM and FC-10/DDM micelles, possibly coupled to the interactions of the C-terminus.

To investigate the protein conformation in the other detergent conditions, backbone assignments in DM and DDM/FC-10 micelles were compared to the chemical shifts observed in the  $^{15}\text{N}$ ,  $^1\text{H}$ -TROSY spectra of detergent conditions in which line broadening impeded obtaining 3D spectra for assignments and structure determination. If it is assumed that cross peaks with similar chemical shifts are the same in different detergent conditions, the observable resonances in DDM and FC-10 are distributed throughout the protein sequence. Cross peaks in the entire C-terminus and both  $\alpha$ -helices were observed under all detergent conditions, consistent with previous evidence that TM0026 is  $\alpha$ -helical, monomeric, and not aggregated in DDM and FC-10<sup>1</sup> and that the observed line broadening is due to exchange processes. However, resonances in the loop, at the C-terminal end of the first  $\alpha$ -helix, and the tertiary contact (A13 determined from the EPR data) were not identified and/or observed under DDM and FC-10 detergent conditions. Therefore, the exchange effects contributing to line broadening do not seem to be localized to one region of TM0026.

In addition, the interactions between the protein and detergents can be mapped by use of the  $^{15}\text{N}$ -resolved  $^1\text{H}$ ,  $^1\text{H}$ -NOESY for the DM and DDM/FC-10 mixed micelles (Figure S9 in Supporting Information).<sup>25,26</sup> For DDM/FC-10, NOEs with the detergent alkyl chain were observed for both transmembrane  $\alpha$ -helices (L7–R27 and F34–V53) and rapid exchange with water was observed for residues in the loop and C-terminus. The cartoon of TM0026 in Figure 6 is colored according to the observed NOEs between the backbone and the alkyl chain of the detergents. A similar trend was observed with DM; however, the assignment was not as comprehensive (see Experimental Section).

(23) Gao, G.; Williams, J. G.; Campbell, S. L. *Methods Mol. Biol.* **2004**, 261, 79–92.

(24) Zuiderweg, E. R. *Biochemistry* **2002**, 41, 1–7.

(25) Fernandez, C.; Hilty, C.; Wider, G.; Wüthrich, K. *Proc. Natl. Acad. Sci. U.S.A.* **2002**, 99, 13533–13537.

(26) Lee, S.; Kim, Y. *FEBS Lett.* **1999**, 460, 263–269.

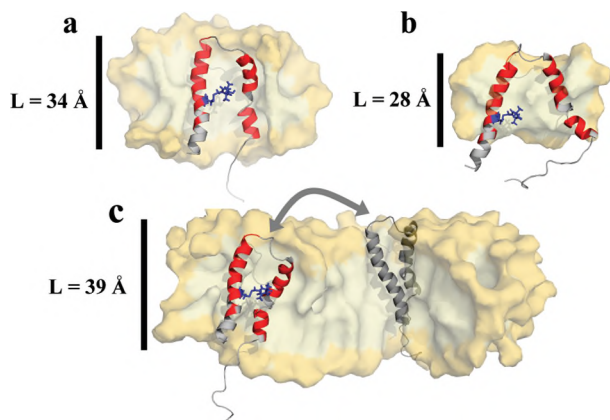


**Figure 6.** Models of matching micelle size and shape to the hydrophobic surface of TM0026. (a) Model demonstrating hydrophobic matching between the hydrophobic dimensions of the protein (hydrophobic length of the  $\alpha$ -helices is  $\approx 29$ – $31$  Å) and the detergent alkyl chains such as in the case of DM, FC-12, and the 4:7 DDM/FC-10 mixed micelle. (b) Model demonstrating a hydrophobic mismatch between the surface area of the protein and the micelles, which are too small, such as in the case of FC-10, causing the  $\alpha$ -helices to separate in order to bury more surface area in the interior of the micelle. (c) Possible model for the heterogeneity observed in the DDM larger micelle. The tertiary fold of the protein is maintained, but there are many regions of the micelle that may accommodate the protein. Another protein molecule is shown in gray for which the hydrophobic surface area of the protein is buried within the micelle, and an arrow indicates exchange between the two conformers. Approximately 25% of the detergent micelle is removed in order to view the protein and the interior of the micelle. The micelle is rendered as a surface and colored yellow. The protein is displayed as a cartoon model; residues for which NOEs between the amide proton and the alkyl chain of detergent molecules are observed are colored red, and residues that were unassigned or lacked NOEs with the detergent are colored gray. The A13R1 side chain is rendered as blue sticks. The dominant headgroup separation  $L$  is labeled in each panel.

### Influence of Micelle Dimensions on Protein Conformations.

The results for TM0026 protein–detergent complexes suggest that the protein conformations are strongly influenced by the size and thickness of the detergent micelle. In interpreting these results, we need to consider that the aggregation number  $N$  can be different for “empty” micelles and micelles in protein–detergent complexes.<sup>15</sup> Similarly, we expect the micelle thickness  $L$  to show some variability in the presence of a protein due to the fluid nature of detergent micelles. Nonetheless, the characteristic headgroup–headgroup dimension  $L$  measured for micelles in the absence of proteins appears to reflect an intrinsic packing preference of the detergent and we observe a similar thickness in TM0026 complexes that yield well-resolved NMR spectra (Figure S6 in Supporting Information).

Taken together, the results suggest that well-resolved NMR spectra are observed when the hydrophobic component of  $L$  (which is equal to  $L$  minus the thickness of the headgroup,  $\approx 29$ – $31$  Å; see Table S3 and Figure S5c in Supporting Information) matches the length ( $\approx 30$ – $33$  Å) of the hydrophobic part of the  $\alpha$ -helices of TM0026 (Figure 6a). We note that this hydrophobic dimension matches the average hydrophobic thickness of the *T. maritima* bilayer ( $\approx 30$  Å<sup>27,28</sup>). In the case of the FC-10 micelle,  $L$  is too small (Table 1). A possible explanation for the observed loss of tertiary interaction and

structural heterogeneity in FC-10 is that the mismatch between the hydrophobic surface and the micelle dimensions may result in a perturbation of the protein structure to avoid hydration of the hydrophobic  $\alpha$ -helices (Figure 6b). This structural perturbation is reminiscent of that observed in the case of “hydrophobic mismatch” observed in lipid bilayers<sup>29</sup> and interhelical packing disruption observed in detergents.<sup>30–32</sup> For the case of DDM, the dominant headgroup separation is larger than the length of the hydrophobic  $\alpha$ -helices, but there is sufficient hydrophobic core volume to accommodate the protein hydrophobic surface area. The protein tertiary structure is maintained in DDM, but line broadening in both the NMR and EPR suggests structural heterogeneity and/or conformational exchange. One of many possible explanations is exchange between protein conformers (for which the tertiary structure is maintained) within a micelle (Figure 6c). For instance, if it is assumed that the protein does not perturb the micelle, the protein cannot traverse the center of the micelle. Instead, the protein may pack in regions of the large micelle that better match the hydrophobic regions of the protein. These allowed environments may be heterogeneous and/or two or more conformers could be in exchange, which would give rise to the observed line broadening in the NMR and EPR spectra. More experiments need to be performed to understand the effects of the detergent on the protein structure that give rise to the observed line broadening in the DDM micelle.

### Conclusion

Using NMR, EPR, and SAXS, we demonstrate a correlation between the dimensions of detergent micelles and the structure of a membrane protein, which leads to the rational design of mixed micelles that facilitates NMR structure determination. In particular, we found that the micelle thickness of mixed micelles depends linearly on the mixing ratio for a significant range of detergent mixtures and that this thickness appears to correlate strongly with the quality of NMR observations.

The generality of the dependence of tertiary contact stability on micelle thickness is difficult to assess at this point, as only very few polytopic membrane protein NMR structures have been determined (seven structures, out of which only one is  $\alpha$ -helical).<sup>33</sup> However, our observations are in qualitative agreement with previous findings. The structure of the glycophorin A dimer (with a similar hydrophobic thickness as TM0026) was solved in FC-12.<sup>34</sup> In sodium dodecyl sulfate (SDS), which has a slightly larger  $L$  value of  $\approx 36$  Å (J.L. and S.D., unpublished results), dimerization is still possible but significantly reduced compared to FC-12.<sup>31</sup> Therien and Deber<sup>30</sup> found that a helix–loop–helix construct from cystic fibrosis transmembrane conductance regulator, which has a shorter hydrophobic thickness compared to glycophorin A and TM0026, dimerizes in micelles with short alkyl chains, while the dimer interaction is predominantly lost in SDS and other micelles of similar thickness.

Future work will explore whether similar relationships can be observed for different membrane proteins varying by size (in particular, larger helical bundles with larger hydrophobic

(27) Eshaghi, S.; Niegowski, D.; Kohl, A.; Martinez Molina, D.; Lesley, S. A.; Nordlund, P. *Science* **2006**, *313*, 354–357.

(28) Lunin, V. V.; Dobrovitsky, E.; Khutoreskaya, G.; Zhang, R.; Joachimiak, A.; Doyle, D. A.; Bochkarev, A.; Maguire, M. E.; Edwards, A. M.; Koth, C. M. *Nature* **2006**, *440*, 833–7.

(29) Killian, J. A. *Biochim. Biophys. Acta* **1998**, *1376*, 401–415.

(30) Therien, A. G.; Deber, C. M. *J. Biol. Chem.* **2002**, *277*, 6067–6072.

(31) Fisher, L. E.; Engelman, D. M.; Sturgis, J. N. *J. Mol. Biol.* **1999**, *293*, 639–651.

(32) Bowie, J. U. *Nature* **2005**, *438*, 581–589.

(33) Raman, P.; Cherezov, V.; Caffrey, M. *Cell. Mol. Life Sci.* **2006**, *63*, 36–51.

(34) MacKenzie, K. R.; Engelman, D. M. *Proc. Natl. Acad. Sci. U.S.A.* **1998**, *95*, 3583–3590.

surface area), fold, and origin. Likely, other micelle properties (such as the total micelle volume) will have to be taken into account to fully understand protein–detergent interactions.

Nonetheless, our data suggest that, rather than exhaustively screening a multitude of detergents, it might be possible to rationally engineer appropriate mixed micelles for NMR structure determination following simple principles and from a limited set of detergents.

**Acknowledgment.** We thank Professor Wayne L. Hubbell for the use of a Varian EPR spectrometer; Professor Kurt Wüthrich for support; Drs. Gerard Kroon, Bernhard Geierstanger, and David Jones for helpful discussion and technical NMR assistance; Dr. Cameron Mura for useful discussions; and Vincent Chu, Dmitri Pavlichin, and Dr. Sönke Seifert for data collection assistance at

the APS. Support for this research was provided by National Institutes of Health Grants 1F32GM068286 and The Jeffress Memorial Trust (L.C.) PO1 GM0066275 (S.D.), and Protein Structure Initiative Grants P50 GM62411 and U54 GM074898 (S.L.). Use of the Advanced Photon Source was supported by the U.S. Department of Energy, Office of Science, Office of Basic Energy Sciences, under Contract DE-AC02-06CH11357. A.Y.L.S. is supported by A\*STAR, Singapore.

**Supporting Information Available:** Further details of SDSL, SAXS, and NMR results. This material is available free of charge via the Internet at <http://pubs.acs.org>.

JA808776J